Journal of Magnetism and Magnetic Materials 323 (2011) 2070–2075

Contents lists available at ScienceDirect

Journal of Magnetism and Magnetic Materials

journal homepage: www.elsevier.com/locate/jmmm

Magnetoelastic properties of $GdMn_6Sn_6$ intermetallic compound

Sh. Tabatabai Yazdi [a], N. Tajabor [a,*], M. Behdani [a], M. Rezaee Roknabadi [a], D. Sanavi Khoshnoud [b], F. Pourarian [c]

[a] Department of Physics, Faculty of Sciences, Ferdowsi University of Mashhad, Mashhad 91775-1436, Iran
[b] Department of Physics, Faculty of Sciences, Semnan University, Semnan, Iran
[c] Department of Materials Science & Engineering, Carnegie Mellon University, Pittsburgh, PA 15219, USA

ARTICLE INFO

Article history:
Received 20 December 2010
Received in revised form
12 February 2011
Available online 12 March 2011

Keywords:
Rare-earth intermetallic compound
Magnetic phase transition
Magnetostriction
Thermal expansion

ABSTRACT

We studied the thermal expansion and magnetostriction of polycrystalline samples of $GdMn_6Sn_6$ intermetallic compound with hexagonal $HfGe_6Fe_6$-type structure in the temperature range of 77–520 K. The thermal expansion measurement of the sample shows anomalous behavior around its $T_C=434$ K and $T_M=309$ K, possibly the point of collapse-like reduction of Mn moments. In addition, the isofield curves of anisotropic and volume magnetostriction reveal anomalies around paramagnetic to ferrimagnetic phase transition. The obtained experimental results are discussed in the framework of two-magnetic sublattices by bearing in mind the lattice parameter dependence of interlayer Mn–Mn exchange interaction in this layered compound. From the temperature dependence of magnetostriction values and considering the magnetostriction relation of a hexagonal structure, we attempt to determine the signs of some of the magnetostriction constants as well as a comparison of their orders of magnitude for this compound.

1. Introduction

The intermetallic compounds with rare-earth and transition metal elements have attracted considerable attention owing to their unusual magnetic properties. Recently, the RMn_6Sn_6 compounds with R=Sc, Y and rare-earth elements (except for R=Pm, Eu and Yb, whose compounds have never been reported) have been widely studied from various aspects, including crystal structure [1], magnetic [2–4], transport, magnetotransport [5] and magneto–optical properties [6] as well as their electronic structure [7]. The RMn_6Sn_6 compounds with R=Sc, Y, Gd–Tm and Lu crystallize in hexagonal $HfFe_6Ge_6$-type structure with space group P6/mmm (Fig. 1), Hf at 1(a) (0, 0, 0), Fe at 6(i) (1/2, 0, $z\approx1/4$), Ge at 2(c) (1/3, 2/3, 0), 2(d) (1/3, 2/3, 1/2) and 2(e) (0, 0, $z\approx1/3$). This crystal structure can be described as layers of R and Mn atoms alternately stacked along the *c*-axis in the sequence Mn–(R, Sn)–Mn–Sn–Sn–Sn–Mn [5]. The layered RMn_6X_6 and RMn_2X_2 compounds (X=Sn, Ge and Si) have attracted much interest because of competing roles of intra- and interlayer exchange interactions on the magnetic structure. The magnetic structure of these compounds consists of two different subsystems: the R and Mn subsystems. the observed complex magnetic properties of these compounds originate from the complicated interplay among the Mn–Mn, R–Mn and R–R exchange interactions as well as the competing magnetocrystalline anisotropies of the two sublattices. The Mn–Mn intralayer direct exchange interaction is positive and strongest which determines the magnetic ordering temperature of these compounds [8]. The interlayer Mn–Mn interactions are one order of magnitude weaker; the coupling through Mn–Sn–Sn–Sn–Mn is always positive (ferromagnetic) while the nature of that within the Mn–(R, Sn)–Mn slab depends on the R element. It is believed that the interlayer Mn–Mn interaction depends strongly on the Mn–Mn interatomic distances, primarily within the layer, i.e. lattice parameter *a* (for larger distances, coupling is usually positive, while for smaller ones it is negative) [9]. The R–Mn indirect interaction in compounds with heavy rare-earth elements (R=Gd, Tb and Dy) has the same order of magnitude as the interlayer Mn–Mn interaction. The R–R RKKY-type coupling is the weakest [9,10]. The R–Mn coupling energy is proportional to $J_{R-Mn}M_RM_{Mn}$ (J is the exchange coupling parameter and M is the saturation magnetization), which in turn is proportional to $(g-1)<J>_RM_{Mn}$ (g factor of the R component) [11]. The quantity $(g-1)J$ is the largest for R=Gd and falls off rapidly towards both ends of the lanthanide series ($J_{Gd-Mn}=-0.93$ meV and $g=2$ [12]). Therefore the R−Mn coupling, being negative for heavy R compounds, is the strongest for $GdMn_6Sn_6$. This compound has the largest lattice parameter of the existing family of RMn_6Sn_6 compounds with $HfFe_6Ge_6$-type structure [1] (so large that the Mn–Mn exchange interaction will not change its sign due to thermal contraction). So, the Mn sublattice is in a ferromagnetic state in the whole ordered range. From magnetization measurements [2] and neutron

* Corresponding author. Tel.: +98 511 8817741; fax: +98 511 8763647.
E-mail addresses: tajabor@ferdowsi.um.ac.ir, ntajabor@yahoo.com (N. Tajabor).

0304-8853/$ - see front matter © 2011 Elsevier B.V. All rights reserved.
doi:10.1016/j.jmmm.2011.03.014

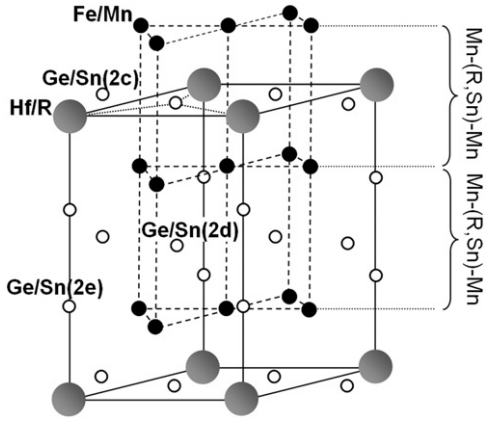

Fig. 1. Representation of $HfFe_6Ge_6$-type crystal structure of RMn_6Sn_6 compounds.

diffraction experiments [3], it was suggested that Gd and Mn sublattices order simultaneously (as a result of strong R–Mn coupling) at about 435 K, i.e. in spite of the presence of two magnetic atoms, $GdMn_6Sn_6$ undergoes a single paramagnetic–ferrimagnetic transition at about T_C=435 K. Since Gd^{3+} is an S-state ion and has no orbital momentum (L=0), the contribution of the Gd sublattice to the magnetic anisotropy of the compound is rather small. So the magnetic anisotropy of $GdMn_6Sn_6$ is governed mainly by the Mn sublattice, which has easy-plane anisotropy, as has been found for RMn_6Sn_6 compounds with non-magnetic elements R=Sc, Y and Lu [3]. Therefore $GdMn_6Sn_6$ favors easy-plane anisotropy in the whole range of the ordered state, with no spin reorientation process.

The magnetic transition in this compound involves transition from the unordered arrangement of Mn moments to the parallel one. Because of the strong interatomic distance dependence of Mn–Mn interlayer interactions, one may expect that this transition is likely to be accompanied by anomalies in the thermal expansion as well as magnetostriction measurements. To date, no report has been published on magnetoelastic properties of RT_6X_6 family (T=Mn, Fe and X=Ge, Sn). Therefore, in the present work, we investigate the spontaneous and field-induced magnetovolume effects in the $GdMn_6Sn_6$ compound by performing linear thermal expansion and magnetostriction measurements.

2. Experiments

The $GdMn_6Sn_6$ polycrystalline samples were prepared by arc melting of the constituent elements under high-purity Ar atmosphere in a water-cooled copper hearth. The raw materials used were of at least of 99.9% purity. The ingots were turned over and re-melted several times to ensure homogeneity. The synthesized ingots wrapped in a tantalum foil were sealed in an evacuated quartz tube, annealed at 1023 K for 4 weeks and then quenched in water to obtain single-phase materials. The purity and microstructure of the prepared samples were checked using X-ray powder diffraction (XRD) with monochromatic Cu Kα radiation ($\lambda\sim$1.5406 Å) in the 2θ range of 20–90° in a continuous scan mode with a step width of 0.05° and scanning electron microscopy (SEM;Leo 1450VP, Carl Zeiss SMT, Germany). For structural characterization, the analysis of the obtained XRD profile was performed using the Fullprof software, which is based on the Rietveld method. In order to reveal the magnetic phase transitions, the thermomagnetic measurement was carried out using a LakeShore 7000 magneto-susceptometer with an ac magnetic field of 50 A/m peak value at 125 Hz in the temperature range of 77–330 K. The linear thermal expansion TE normalized to 77 K ($\Delta l/l=(l_T-l_{77\ K})/l_{77\ K}$) and magnetostriction (MS) were measured using the strain-gage Wheatstone bridge technique on disk-shaped samples with a diameter of about 6 mm and thickness of about 2 mm in the temperature range of 77–520 K and magnetic fields up to 1.5 T. The accuracy of these measurements was better than 2×10^{-6}. The longitudinal ($\lambda_\parallel$) and transverse magnetostriction ($\lambda_\perp$) of the samples were measured parallel and perpendicular to the applied magnetic field, respectively. The anisotropic magnetostriction (λ_t) and volume magnetostriction (ω) were calculated directly from the relations $\lambda_t=\lambda_\parallel-\lambda_\perp$ and $\omega=\lambda_\parallel+2\lambda_\perp$.

3. Results and discussion

The XRD patterns indicate that the samples are highly pure and single-phase with $HfFe_6Ge_6$-type structure (S.G. P6/mmm) containing a small amount of β-Sn, Gd_2O_3 and Mn_3Sn_2. The presence of such minor impurity phases has been reported in most previous attempts to prepare RMn_6Sn_6 samples by arc-melting or solid-state reaction method, for instance Refs. [13,14]. The refined lattice parameters using the Reitveld analysis are a=5.54671 Å, c=9.04348 Å the corresponding unit-cell volume V=240.956 Å^3 and c/a=1.6304, which are quite close to the reported values in the literature [15]. Fig. 2 displays the result of the Reitveld refinement. The SEM microstructural analysis revealed that the samples consist mainly of large grains of $GdMn_6Sn_6$ phase and the minor impurity phases in the grain boundaries, consistent with the XRD results.

The ac magnetic susceptibility χ_{ac} of the studied sample in a zero dc magnetic field in the temperature range of 77–330 K (not presented here) is characterized by a non-linear increase of magnetization and, as expected, without any ordering point in this temperature range.

Fig. 3 shows the temperature dependence of the zero-field linear thermal expansion dl/l of the studied sample in the range of 77–520 K. It displays a metallic behavior with a shallow anomaly near T_C=434 K (precisely the curie temperature obtained previously from magnetization and neutron diffraction measurements [2,3]), along with a change of slope at about T_M=309 K. The small anomaly, that thermal expansion shows near T_C is better observed in the temperature dependence of the thermal expansion coefficient α of the sample, depicted graphically by taking a point-to-point temperature derivative of the dl/l data. The occurrence of the positive volume anomalous behavior observed upon the ferri- to paramagnetic transition can be explained as follows: the loss of ferrimagnetism on heating through T_C leads to a decrease in the number of nearest R–Mn neighbors with the indirect 4f–5d–3d exchange interaction and antiparallel spins (and therefore attraction interaction) and hence the crystal volume increases. It is worth noting that this volume change being continuous at T_C indicates a second-order ferri–paramagnetism transition. For the anomalous behavior (noticeable volume expansion) observed around T_M, we have no well-based explanation; one possibility needing further investigation is the collapse-like reduction of ferromagnetic Mn moments at this temperature, consistent with the thermal variation of Mn moments in this compound reported previously [3]. With increasing temperature from low values, the Gd moment decreases gradually from μ_{Gd}=6.5 μ_B down to about 5.5 μ_B at 300 K while μ_{Mn}=2.4 μ_B remains constant and exhibits no visible change in this temperature span. Then in a narrow temperature range above 300 K, the Mn moment drops significantly. This behavior is consistent with the Jaccarino and Walker (JW) model [16]. According to this model, the local moment on a transition metal atom is critically dependent on the number and type of its nearest

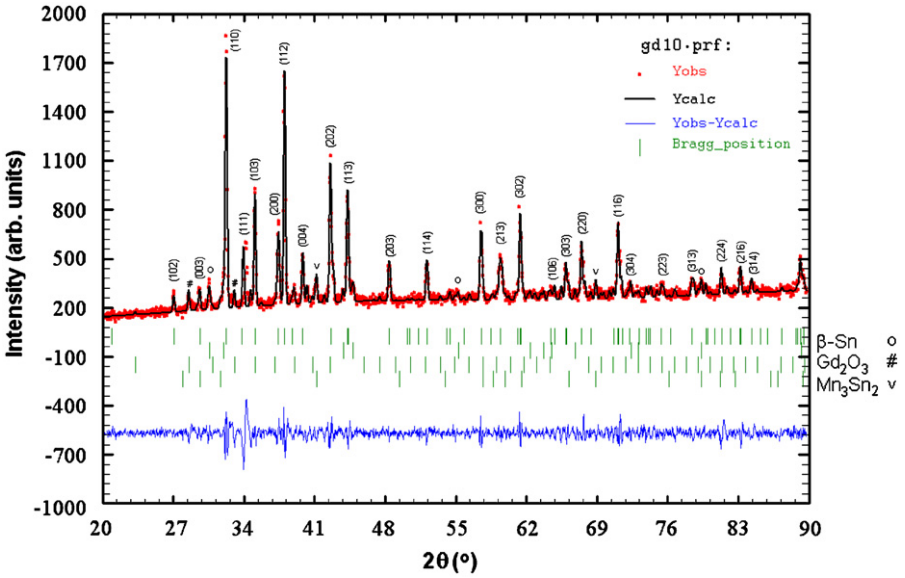

Fig. 2. Observed (circles) and calculated (solid lines) XRD pattern of the $GdMn_6Sn_6$ sample at room temperature. Vertical bars indicate the position of Bragg reflections (upper tiks mark $GdMn_6Sn_6$ lines and the lower ones belong to impurity phases). Difference between the observed and calculated intensities is given at the bottom of the diagram.

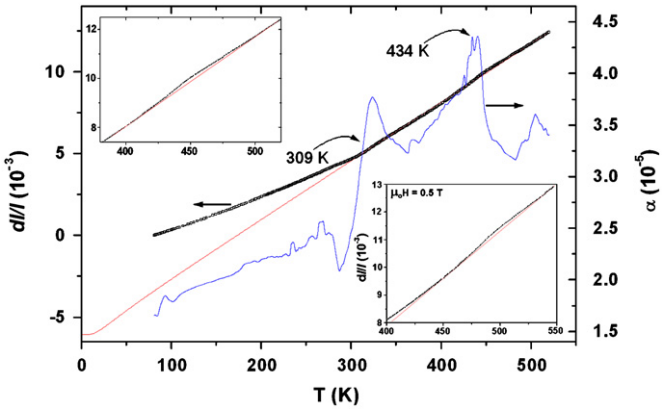

Fig. 3. Temperature dependence of the linear thermal expansion and thermal expansion coefficient α versus temperature for $GdMn_6Sn_6$ sample (the anomalous thermal expansion behavior in the T_C region is enlarged in the upper left inset). The dashed line shows the simulated phonon contribution (Grüneisen law) using $\theta_D=102$ K. The lower right inset is the temperature dependence of the thermal expansion under the applied magnetic field of 0.5 T.

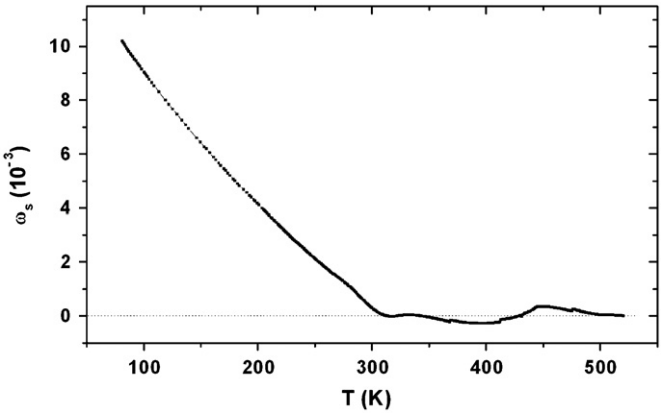

Fig. 4. Temperature dependence of the spontaneous volume magnetostriction ω_s.

neighbor atoms. It means that the temperature dependence of the Mn moment depends on the Mn–Mn interatomic distances. As no well-defined anomaly is found in $\chi_{ac}(T)$ measurements at T_M (as in the $GdMn_2$ compound [17]), one can propose a Gd canted and Mn antiferromagnetic structure (GCMA model), where the Gd moments are canted with each other in Gd sites and the Mn moments couple antiferromagnetically to each other in their sublattice. If one is to accept this model, it should be noted that it is meta-stable when a magnetic field is applied. The thermal expansion measurement under the applied magnetic field of 0.5 T confirms this statement (inset of Fig. 3). Finally, an additional minor anomaly appearesd above 500 K in the α behavior of the sample. We have no well-based explanation for this anomaly located in the paramagnetic regime. We do not expect any inherent anomalous behavior of either $GdMn_6Sn_6$ or of the existing identified minor phases in this range of temperature. It is possibly due to the systemic errors in high temperature measurements (close to the maximum temperature limit of the used strain gage and the solder).

The magnetic contribution to the thermal expansion $(dl/l)_m$ can be estimated from the difference between the observed dl/l curve and the usual anharmonic phonon contribution governed by the Grüneisen law. According to this empirical law $\alpha(T)=\gamma\kappa_T C_v(T)/3$, where Grüneisen parameter γ and isothermal compressibility coefficient κ_T are relatively insensitive to the temperature. Therefore, the TE coefficient α and the specific heat C_v have essentially a linear relationship. Since contribution from electronic subsystem is negligible in comparison with the magnetic and lattice ones, the difference between the observed TE and the phonon one is due to the magnetic interactions. We derived the phonon contribution from the Debye elementary model with $\theta_D=102$ K [18]. The calculated nonmagnetic contribution that has been fitted to the experimental results in the paramagnetic regime is depicted in Fig. 3 as a dashed line. Assuming that the linear thermal expansion dl/l is isotropic, the spontaneous volume magnetostriction is $\omega_s=3(dl/l)_m$. The temperature dependence of the ω_s values is shown in Fig. 4. The insignificant spontaneous magnetostriction

effects in the paramagnetic phase should be due to the existence of short-range magnetic correlations above the ordering temperature.

For further discussion on the observed spontaneous magneto-volume effects in this compound, we apply a phenomenological theory stating that the extra contribution to the thermal expansion over the lattice one is caused by a change in the magnitude of local moments and also by a change in the relative orientations of the neighboring ones [19]. It means that magnetic volume change is composed of two contributions: a band term proportional to the square amplitude of the local spin fluctuations or in other words, the square of the local moments (longitudinal spin fluctuations or Stoner excitations [20]) and an interaction term proportional to the pair correlation function between local moments (transverse spin fluctuations or spin-wave excitations). Therefore, ω_s in a two-sublattice model of this intermetallic compound can be described as follows [21]:

$$\omega_s = n_{\mathrm{Mn-Mn}}\mu_{\mathrm{Mn}}^2 + n_{\mathrm{Mn-Gd}}\mu_{\mathrm{Mn}}\mu_{\mathrm{Gd}} + n_{\mathrm{Gd-Gd}}\mu_{\mathrm{Gd}}^2 \quad (1)$$

where $n_{\mathrm{Mn-Mn}}$ and $n_{\mathrm{Gd-Gd}}$ are the magnetoelastic-coupling coefficients in the Mn and Gd sublattices, respectively, and $n_{\mathrm{Mn-Gd}}$ is the intersublattice coupling coefficient ($n_{3d-3d} \gg n_{3d-4f} \gg n_{4f-4f}$). The last term is known to be negligible in intermetallics with a high 3d metal content [22]. From the low value of ω_s in the T_C region, we conclude that the transverse spin fluctuations of Gd magnetic moments are the main origin of volume effects in this region, whereas the large ω_s values at $T < T_M$ can be ascribed to the longitudinal spin fluctuations.

Now discussing the Mn moment collapse at T_M, it should be mentioned that, considering a linear relation between $n_{\mathrm{Mn-Mn}}$ and the unit cell dimensions [23], a volume change of more than 10% would be expected if the Mn moment of 2.4 μ_B collapsed completely at T_M. The observed value of about 1% suggests that the Mn moment does not collapse to zero at T_M, but remains finite due to spin fluctuations.

A discussion on the volume effects around T_C is given by Bozorth [24] in terms of the Bethe–Slater curve representing the exchange energy as a function of R/r (the ratio of the atomic radius to the radius of the incomplete shell responsible for magnetism) with a maximum value at a certain R/r. As found from Fig. 3, the $GdMn_6Sn_6$ sample expands upon heating through T_C, or, in other words, it possesses a greater α in the ferromagnetic state than in the paramagnetic one, i.e. decrease of exchange integral in this compound is accompanied by an increase in its R/r value. This implies that the $GdMn_6Sn_6$ compound must lie to the right of the maximum of the Bethe's interaction curve, consistent with the ferrimagnetic order of this compound. The rather high R/r value for $GdMn_6Sn_6$ may be expected, since the 4f shell of Gd is buried rather deeply within the structure of the atom (Gd in particular has the maximum value of $r_R - r_{4f}$ in the 4f series [25], leading to a large R_{Gd}/r_{4f}). In addition, the Mn atoms in the compound are farther apart than in the pure Mn metal, therefore leading to a rather large R_{Mn}/r_{3d}.

The longitudinal $\lambda_\parallel$, transverse $\lambda_\perp$, anisotropic λ_t and volume magnetostriction ω isotherms as a function of the applied magnetic field at some selected temperatures are presented in Fig. 5. At first glance it is observed that $\lambda_\parallel$ is negative and roughly three times larger and opposite in sign compared to $\lambda_\perp$, leading to a considerable anisotropic magnetostriction. For all temperatures except those around T_C, both $\lambda_\parallel(H)$ and $\lambda_\perp(H)$, as well as the calculated $\lambda_t(H)$, increase strongly in low fields and then tend towards saturation. The observed abrupt change of magnetostriction (because of the enhanced magnetization) in the low field region can be attributed to the conventional domain extension relevant to the domain-wall motion in the ferrimagnetic state. In addition, it is clear from Fig. 5 that, except for temperatures in the vicinity of T_C, the saturation behavior of the magnetostriction occurs at threshold magnetic fields H_{th} not differing significantly for different temperatures. The low and almost temperature-independent values of H_{th} indicate the easy movement of domain-walls and absence of any pinning center in the studied compound. Generally, in rare-earth/transition metal intermetallic compounds, the local 4f orbitals of the rare-earth atoms creating large magnetocrystalline anisotropy are responsible for providing strong pinning centers [26]. However, this is not the situation in the present compound with R≡Gd being an S state ion (L=0) with a spherical symmetric 4f charge density and so unaffected by

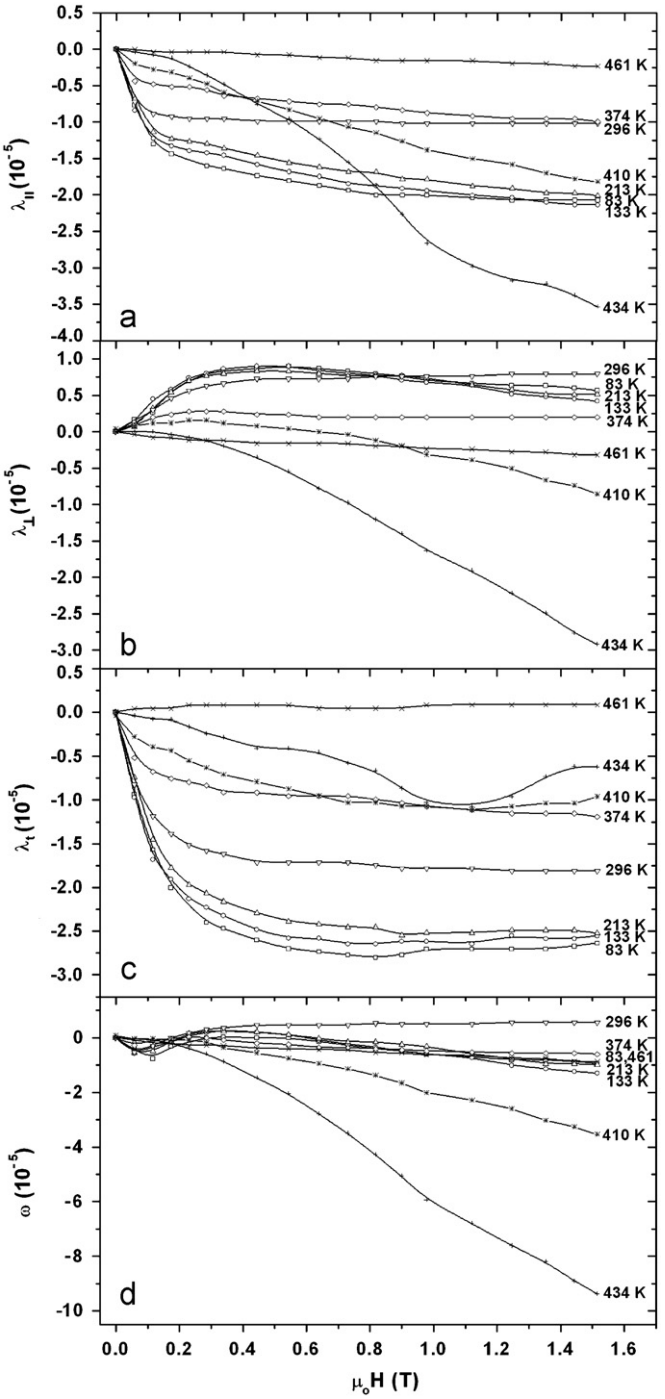

Fig. 5. (a) Longitudinal $\lambda_\parallel$, (b) transverse $\lambda_\perp$, (c) anisotropic λ_t and (d) volume magnetostriction ω isotherms of the $GdMn_6Sn_6$ sample versus applied magnetic field at some selected temperatures. In this and the following figures, the lines connecting the data points are only guides for the eye.

the crystal field. In Gd, the spin magnetic moments are free to assume any direction in space dictated by other factors such as applied magnetic field. By increasing the applied magnetic field through H_{th}, as well as domain extension, the magnetic moments gradually rotate towards the field direction, i.e. the magnetic field forces the linear ferrimagnetic ordering of the $GdMn_6Sn_6$ compound to the nonlinear one. This rotation of antiparallel Gd- and Mn-sublattice moments is accompanied by considerable volume effects, giving rise to a negative magnetoelastic coupling constant in the direction parallel to the applied magnetic field and positive one in the perpendicular direction (except for temperatures around T_C). However, the high temperature magnetostriction isotherms in Fig. 5, corresponding to the temperatures around T_C, increase continuously with the magnetic field with no sign of saturation, i.e. higher fields are needed for saturation at temperatures in the T_C region (say higher than about 400 K). The isotherm variations for the magnetic field parallel ($\lambda_{\parallel}$) and perpendicular ($\lambda_{\perp}$) to the measurement exhibit a H^2 dependence up to about 1 T, which is the expected behavior of the magnetostriction for the paramagnetic phase at low fields, where susceptibility is field independent.

For volume magnetostriction ω, it is seen from Fig. 5d that, with the exception of the isotherm corresponding to T_C, all the isotherms being initially negative pass through minima and then increase with a positive slope, having sign reversal. These extrema probably originate from an extremum in the local magnetic anisotropy, leading to the collective rotation of the Mn moments towards the applied magnetic field direction. It is worth mentioning that no field-induced transition is observed upon applying magnetic fields up to 1.5 T. This was expected, as due to the strong Gd–Mn exchange coupling ($J_{Gd-Mn}/k_B = -10.7$ K [15]) the Gd- and Mn-sublattice moments remain strictly antiparallel at magnetic fields available in this work.

Fig. 6 shows the temperature dependence of the anisotropic magnetostriction λ_t at some typical applied magnetic fields up to 1.5 T. As seen, λ_t is almost field-independent and, apart from an anomalous behavior around 423 K (close to T_C of the sample), from $|\lambda_t| \sim 3\times10^{-5}$ at low temperatures drops continuously to zero at temperatures above T_C owing to the natural decrease of magnetization due to thermal fluctuations. This is somewhat the typical behavior of the anisotropic magnetostriction of a ferromagnetic compound, indicating the weakening of the ferromagnetic coupling of Mn moments.

For further discussion we consider the phenomenological relation of magnetostriction for a hexagonal structure describing the strain measured in a direction with cosines β_i ($i=x, y, z$) when magnetization is in a direction described by cosines α_i ($i=x, y, z$),

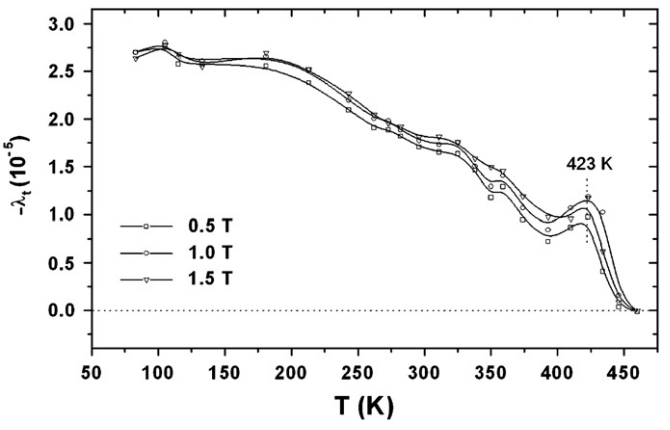

Fig. 6. Temperature dependence of the anisotropic magnetostriction of the $GdMn_6Sn_6$ sample at the selected magnetic fields of 0.5, 1.0 and 1.5 T.

following the standard theory of Callen and Callen [27]:

$$\lambda = \tfrac{1}{3}\lambda_{11}^{\alpha} + \tfrac{1}{2}\sqrt{3}\lambda_{12}^{\alpha}(\alpha_z^2 - \tfrac{1}{3}) + 2\lambda_{21}^{\alpha}\left(\beta_z^2 - \tfrac{1}{3}\right) + \sqrt{3}\lambda_{22}^{\alpha}\left(\beta_z^2 - \tfrac{1}{3}\right)(\alpha_z^2 - \tfrac{1}{3}) + 2\lambda^{\gamma}\left\{\tfrac{1}{4}(\beta_x^2 - \beta_y^2)(\alpha_x^2 - \alpha_y^2) + \beta_x\beta_y\alpha_x\alpha_y\right\} + 2\lambda^{\varepsilon}(\beta_x\alpha_x + \beta_y\alpha_y)\beta_z\alpha_z \quad (2)$$

Here the magnetostrictive coefficients $\lambda_{jj'}^{\Gamma}(T, H)$ are deformations originating either from the single-ion crystal electric field interaction (λ_{12}^{α}, λ_{22}^{α}, λ^{γ} and λ^{ε}), or from the two-ion exchange interaction (λ_{11}^{α} and λ_{21}^{α}). The modes with the superscript $\Gamma=\alpha$ indicate the fully symmetric volume change preserving the hexagonal structure, and $\Gamma=\gamma$ and ε ones represent shearing strains in the basal plane and in planes parallel to the c-axis, respectively. The first subscript j denotes the degree of measurement direction cosines pertaining to that particular term, i.e. the second superscript, i.e. λ_{1j}^{α}, ($j'=1, 2$) coefficients are the terms independent of measurement direction (the basal plane volume modes) and $\lambda_{2j'}^{\alpha}$ ones are quadratic in α_i (the longitudinal volume modes). The second subscript j' relates to the degree of magnetization direction cosines exactly in the same way. In a single crystal sample all $\lambda_{jj'}$ coefficients are responsible for the different types of deformation and distortion, while for a polycrystalline sample, the MS expression must be averaged over all directions within a sphere. Following Mason [28], we calculate the λ_t expression for a polycrystalline hexagonal sample to be

$$\lambda_t = \lambda_{\parallel} - \lambda_{\perp} = \frac{2\sqrt{3}}{15}\lambda_{22}^{\alpha} + \frac{2}{5}(\lambda^{\gamma} + 2\lambda^{\varepsilon}) \quad (3)$$

where λ_{22}^{α} mode is associated with a longitudinal change in the c/a ratio for the fixed volume upon the magnetization rotation from the basal plane to the c-axis. This mode maintains the hexagonal symmetry. The λ^{γ} and λ^{ε} modes refer to a shear breaking of the circular symmetry of the basal plane by magnetization rotation in the plane and a shear tilting the c-axis, respectively. Notice that no exchange striction terms are present at all in the λ_t expression for the present sample being an easy plane compound with high anisotropy field (≈ 9 T [29]), the magnetization rotation in low temperatures and fields is restricted to the basal plane. Therefore, bearing all the above in mind, λ^{γ} is the dominant term under the conditions of low temperatures and fields. Hence, from the outline presented here, one can conclude that λ^{γ} is negative for this compound. As temperature increases the planar anisotropy field decreases because of the decrease of the second-order magnetic anisotropy constant K_1 by an absolute value in this compound (K_2 and K_3 appear to depend weakly on temperature) [29]; therefore the magnetization vector senses all directions. This leads λ^{γ} to decrease and tend to zero at T_C. Therefore, from Eq (3) and considering that λ^{ε} can be neglected in easy plane compounds, as for the sample in the present study, we conclude that at higher temperatures λ_{22}^{α}, being the dominant mode in λ_t results, is negative for $GdMn_6Sn_6$. Finally, the reasonable maxima around T_C in λ_t curves can be attributed to the variation of the λ_{22}^{α} mode with temperature.

The temperature dependence of the volume magnetostriction ω at selected applied magnetic fields is presented in Fig. 7. As seen, in contrast to the λ_t behavior, ω depends strongly on the magnitude of the applied field especially in the T_C region. Regardless of the applied magnetic field magnitude, $\omega(T)$ peaks drastically at $T_C = 434$ K (precisely the ferri- to paramagnetic transition point obtained from thermal expansion measurements, Fig. 3, and well consistent with literature). The occurrence of this magnetovolume effect upon the ferri- to paramagnetic transition, can be explained as in the observed thermal expansion anomaly around T_C.

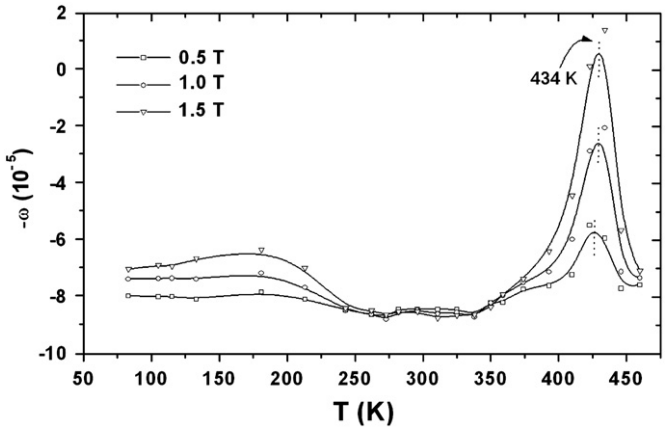

Fig. 7. Temperature dependence of the volume magnetostriction ω of the $GdMn_6Sn_6$ sample at the selected magnetic fields of 0.5, 1.0 and 1.5 T.

For further discussion on volume magnetostriction of this compound (Fig. 7) we calculate the expression for the ω of a hexagonal polycrystalline sample, following a similar procedure as performed for λ_t, as follows:

$$\omega = \lambda_{\parallel} + 2\lambda_{\perp} = \lambda_{11}^{\alpha} \quad (4)$$

So the λ_{11}^{α} coefficient is negative for the $GdMn_6Sn_6$ compound, and the observed maxima at T_C in the ω curves are ascribed to the variation of this mode with temperature. The λ_{11}^{α} mode denoting an expansion or a contraction in the basal plane originates from the two-ion isotropic exchange interaction, which depends only on the distance between ions. This term is dependent only on the magnitude of the magnetization (or the applied magnetic field), and not on its direction. As the anomaly around T_C in ω behavior is observed to be about one order of magnitude larger than the one in the λ_t behavior, one can deduce that the λ_{11}^{α} mode (the contribution of the isotropic two-ion exchange interaction in MS) is about one order of magnitude larger than the λ_{22}^{α} mode (the anisotropic single-ion crystal electric field contribution). It is consistent with the fact that the absolute value of strain caused by two-ion interactions such as exchange striction is one order of magnitude larger than the single-ion one [27].

4. Conclusions

Highly pure single-phase polycrystalline samples of $GdMn_6Sn_6$ intermetallic compound were prepared by the arc melting method. The compound possesses a hexagonal $HfFe_6Ge_6$-type structure (S.G. P6/mmm) with the refined lattice parameters of $a=5.54671$ Å and $c=9.04348$ Å. The magnetostriction and thermal expansion of the samples have been investigated in the temperature range of 77–520 K. The thermal expansion measurements show anomalous behavior around $T_C=434$ K and $T_M=309$ K, which possibly corresponds to the point of collapse-like reduction of Mn moments. The isofield curves of anisotropic and volume magnetostriction peak at the paramagnetic to ferrimagnetic phase transition. The experimental results obtained were discussed in the framework of two-magnetic sublattices by accounting for the lattice parameter dependence of the interlayer Mn–Mn exchange interaction in this layered compound. From the temperature dependence of magnetostriction measurements and considering the magnetostriction relation of a hexagonal structure, the signs of some of the magnetostriction constants for this compound, as well as a comparison of their orders of magnitude, were determined. The results show that the contribution of the isotropic two-ion exchange interaction in magnetostriction is about one order of magnitude larger than the anisotropic single-ion crystal field contribution.

References

[1] B. Malaman, G. Venturini, B. Roques, Mat. Res. Bull. 23 (1988) 1629.
[2] G. Venturini, B. Chafik El Idrissi, B. Malaman, J. Magn. Magn. Matter. 94 (1991) 35.
[3] B. Malaman, G. Venturini, R. Welter, J.P. Sanchez, P. Vulliet, E. Ressouche, J. Magn. Magn. Mater. 202 (1999) 519.
[4] D.M. Clatterbuck, K.A. Gschneidner Jr., J. Magn. Magn. Matter. 207 (1999) 78.
[5] F. Canepa, R. Duraj, C. Lefèvre, B. Malaman, A. Mar, T. Mazet, M. Napoletano, A. Szytula, J. Tobola, G. Venturini, A. Vernière, J. Alloys Compd. 383 (2004) 10.
[6] D.M. Clatterbuck, R.J. Lange, K.A. Gschneidner Jr., J. Magn. Magn. Mater. 195 (1999) 639.
[7] T. Mazet, J. Tobola, G. Venturini, B. Malaman, Phys. Rev. B 65 (104406) (2002) 1.
[8] I.Yu. Gaĭdukova, Gou Guanghua, S.A. Granovskiĭ, I.S. Dubenko, R.Z. Levitin, Phys. Solid State 41 (1999) 1885.
[9] J.H.V.J. Brabers, A.J. Nolten, F. Kayzel, S.H.J. Lenczowski, K.H.J. Buschow, F.R. de Boer, Phys. Rev. B 50 (22) (1994) 16410.
[10] Guo Guang-Hua, Wu Ye, Zhang Hai-Bei, D.A. Filippov, R.Z. Levitin, V.V. Snegirev, Chin. Phys. 11 (2002) 608.
[11] J.H.V.J. Brabers, V.H.M. Dujin, F.R. de Boer, K.H.J. Buschow, J. Alloys Compd. 198 (1993) 127.
[12] P. Tils, M. Loewenhaupt, K.H.J. Buschow, R.S. Eccleston, J. Alloys Compd. 279 (1998) 123.
[13] O. Cakir, I. Dincer, A. Elmali, Y. Elerman, H. Ehrenberg, H. Fuess, J. Alloys Compd. 416 (2006) 31.
[14] G. Venturini, J. Alloys Compd. 400 (2005) 37.
[15] S. Kimura, A. Matsuo, S. Yoshii, K. Kindo, L. Zhang, E. Brück, K.H.J. Buschow, F.R. de Boer, C. Lefèvre, G. Venturini, J. Alloys Compd. 408–412 (2006) 169.
[16] V. Jaccarino, L.R. Walker, Phys. Rev. Lett. 15 (1965) 258.
[17] T. Okamoto, H. Fujii, Y. Makihara, T. Hihara, Y. Hashimoto, J. Magn. Magn. Mater. 54–57 (1986) 1087.
[18] H.G.M. Duijn, Ph.D. Thesis, Universiteit van Amsterdam, 2000, p. 141.
[19] M. Shiga, J. Phys. Soc. Japan 50 (1981) 2573.
[20] P.A. Algarabel, M.R. Ibarra, C. Marquina, S. Yuasa, H. Miyajima, y. Otani, J. Appl. Phys. 79 (1996) 4659.
[21] E.W. Lee, F. Pourarian, Phys. Status Solidi (a) 33 (1976) 483.
[22] A.V. Andreev, in: K.H.J. Buschow (Ed.), Handbook of Magnetic Materials, Vol. 8, North-Holland, Amsterdam, 1995, p. 59.
[23] J.H.V.J. Brabers, C.H. de Groot, K.H.J. Buschow, F.R. de Boer, J. Magn. Magn. Mater. 157/158 (1996) 639.
[24] R.M. Bozorth, Ferromagnetism, D. Van Nostrand Company, Inc., New York, 1951, p. 444.
[25] E. Belorizky, M.A. Fermi, J.P. Gavigan, D. Givord, H.S. Li, J. Appl. Phys. 61 (1987) 3971.
[26] M.R. Alinejad, N. Tajabor, F. Pourarian, J. Magn. Magn. Mater. 320 (2008) 2140.
[27] E. Callen, H.B. Callen, Phys. Rev. 139 (1965) A455.
[28] W.P. Mason, Phys. Rev. 96 (1954) 302.
[29] P.B. Terent'ev, N.V. Mushnikov, V.S. Gaviko, L.A. Shreder, E.V. Rosenfeld, J. Magn. Magn. Mater. 320 (2008) 836.